

# Energy Barriers to Chemical Reactions. Why, How, and How Much? Non-Arrhenius Behavior in Hydrogen Abstractions by Radicals

Andreas A. Zavitsas

Contribution from the Department of Chemistry, Long Island University, Brooklyn, New York 11201

Received October 24, 1997. Revised Manuscript Received April 27, 1998

**Abstract:** Using free-radical hydrogen abstractions of the type  $X-H + \cdot Y \rightarrow X\cdot + H-Y$  as a model for reactions involving simultaneous bond breaking and bond making, we find that the enthalpy of activation may increase or decrease with temperature. This depends on changes in bond dissociation energies and their effect on (a) the enthalpy of reaction and (b) the triplet repulsion between the terminal groups X and Y. The variety of observed curvatures in plots of  $\ln(k)$  vs  $1/T$  for eight typical reactions can be described primarily by these two factors, over temperature ranges greater than 1000 K. The reactions treated are  $OCH_2 + \cdot H$ ,  $CH_4 + \cdot H$ ,  $H_2 + \cdot CH_3$ ,  $C_2H_6 + \cdot CH_3$ ,  $C_2H_6 + \cdot H$ ,  $H_2 + \cdot C_2H_5$ ,  $CH_4 + \cdot Br$ , and  $H_2 + \cdot Br$ .

## Introduction and Background

Rate constants for several reactions have been measured over temperature ranges exceeding 1000 K, with the largest class being gas-phase hydrogen abstractions by radicals. Curvature is often observed in plots of the logarithm of the rate constant vs the reciprocal absolute temperature,  $\ln(k)$  vs  $1/T$ , that is, non-Arrhenius behavior. Experimental data over extended temperature ranges are often described by the three-parameter eq 1,

$$k = aT^n e^{-b/(RT)} \quad (1)$$

where the constants  $a$ ,  $n$ , and  $b$  provide the best fit. There are various approaches to understanding non-Arrhenius behavior.<sup>1</sup> Many focus on the preexponential or entropy term, the effect of temperature on partition functions, and postulated low-frequency bending vibrations at the transition state (TS).<sup>2</sup> Variational TS theory<sup>3</sup> and high-level ab initio calculations,<sup>4</sup> with various types of tunneling corrections applied to the calculated rate constants,<sup>5</sup> have been shown to reproduce non-Arrhenius behavior in some cases. Curvatures of Arrhenius plots for different reactions vary widely, from minimal ( $n \approx 0$  in eq 1) to quite pronounced ( $n = 6$ ). The variability of such curvatures is examined here by an alternative approach, focusing on the energy term. Relevant background is outlined below.

In formulating the expression for attainment of chemical equilibrium in 1884, van't Hoff suggested that the energy difference between reactants and products may not be independent of temperature.<sup>6</sup> For the forward and reverse rate constants he wrote eq 2, where  $E_{-1} - E_1$  is the standard change in internal energy between products and reactants, and considered the two possibilities that the energy change, and therefore  $E_1$  and  $E_{-1}$ ,

$$\begin{aligned} d \ln(k_1)/dT &= E_1/(RT^2) \\ \text{and } d \ln(k_{-1})/dT &= E_{-1}/(RT^2) \quad (2) \end{aligned}$$

be dependent or independent of temperature. For  $E$  independent of temperature, integration of eq 2 gives the 1889 Arrhenius equation,<sup>7</sup>  $k = A e^{-E_a/(RT)}$ , which requires a linear relationship between  $\ln(k)$  and  $1/T$ .

Eyring's 1935 transition-state theory led to eq 3, where  $k_B$

$$k = \kappa(k_B/h)T e^{\Delta S^\ddagger/R} e^{-\Delta H^\ddagger/(RT)} \quad (3)$$

and  $h$  are the Boltzmann and Planck constants, respectively, and  $\Delta S^\ddagger$  and  $\Delta H^\ddagger$  are the changes in entropy and enthalpy on going from the starting state to the TS. The transmission coefficient  $\kappa$  is often approximated as unity.<sup>1,8</sup> The value of  $\kappa$  would tend to decrease if, after the reacting system has successfully crossed the dividing surface between reactants and products, there is reflection back toward reactants. Recrossing would lead to violation of the theory's assumption of equilibrium between reactants and activated complex. Values of  $\kappa > 1$  would be caused by "barrier leakage", for example, tunneling.<sup>8</sup> For chemical reactions under ordinary conditions, the probability of recrossing is not great and there is little effect on  $\kappa$  from this source. Extremely low enthalpies of activation or, the equivalent, very energetic reactants may lead to decreases in  $\kappa$ .<sup>1</sup> Equation 3 produces a linear relationship between  $\ln(k/T)$  and  $1/T$ , but only if  $\Delta S^\ddagger$ ,  $\Delta H^\ddagger$ , and  $\kappa$  are independent of temperature.

Experimentally determined rate constants for some reactions produce linear plots of  $\ln(k)$  vs  $1/T$  (Arrhenius behavior), for others linear plots of  $\ln(k/T)$  vs  $1/T$  are obtained (eq 3 with constant  $\Delta S^\ddagger$ ,  $\Delta H^\ddagger$ , and  $\kappa$ ), and the majority are fitted best by the three-parameter eq 1, proposed by van't Hoff's student Kooij in 1893.<sup>9</sup>

Heitler and London postulated in 1927 that the bonding energy between two atoms is the sum of the Coulombic and

(1) Laidler, K. J. *Chemical Kinetics*, 3rd ed.; Harper and Row: New York, 1987.

(2) Benson, S. W. *Thermochemical Kinetics*; Wiley: New York, 1968.

(3) For an excellent account of the current status of variational transition state theory, see: Truhlar, D. G.; Garrett, B. C.; Klippenstein, S. J. *J. Phys. Chem.* **1996**, *100*, 12771.

(4) For recent examples, see: (a) Rosenman, E.; McKee, M. L. *J. Am. Chem. Soc.* **1997**, *119*, 9033. (b) Bowdridge, M.; Furue, H.; Pacey, P. D. *J. Phys. Chem.* **1996**, *100*, 1676.

(5) Kim, Y.; Kreevoy, M. M. *J. Am. Chem. Soc.* **1992**, *114*, 7116.

(6) van't Hoff, J. H. *Etudes de dynamique chimique*; F. Muller and Co.: Amsterdam, 1884.

(7) Arrhenius, S. *Z. Phys. Chem.* **1889**, *4*, 226–248.

(8) Eyring, H. *J. Chem. Phys.* **1935**, *3*, 107. Wynne-Jones, W. F. K.; Eyring, H. *J. Chem. Phys.* **1935**, *3*, 492. Eyring, H.; Eyring, E. M. *Modern Chemical Kinetics*; Reinhold Publishing Corp.: New York, 1963.

(9) Kooij, D. M. *Z. Phys. Chem.* **1893**, *12*, 155. Laidler, J. K. *The World of Physical Chemistry*; Oxford University Press: Oxford, 1993.

exchange energies and that triplet repulsion (parallel electron spins) is their difference, Coulombic energy minus exchange energy.<sup>10</sup> In 1928, London extended the treatment with serious approximations to H<sub>3</sub> (the TS for the identity hydrogen exchange H:H + •H → H• + H:H).<sup>11</sup> For X:H + •Y → X• + H:Y, the London equation for the TS of the three-electron system is eq 4, where *A* and *α* refer respectively to Coulombic and exchange

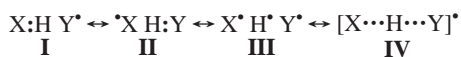
$$E^\ddagger = A + B + C + [1/2\{(\alpha - \beta)^2 + (\beta - \gamma)^2 + (\gamma - \alpha)^2\}]^{1/2} \quad (4)$$

energies between X and H, *B* and *β* to those between H and Y, and *C* and *γ* to those between X and Y. The overlap integral is disregarded in eq 4. In identity exchanges, where X = Y, *A* = *B*, and *α* = *β* because of symmetry and eq 4 simplifies to eq 5.

$$E^\ddagger = (A + \alpha) + (C - \gamma) + A \quad (5)$$

## Method

It is possible to estimate how much of the observed curvature of plots of ln(*k*) vs 1/*T* may be due to changes in the enthalpy of activation, as a result of changes in bond dissociation energies (BDEs or bond enthalpies) with temperature. This work focuses primarily on this point. Gas-phase heats of formation are known over wide temperature ranges for a number of simple molecules and radicals, thus allowing for the calculation of BDEs over such ranges. BDE effects on reaction rates can be estimated by using our calculation method, which is based on intersecting potential energy curves.<sup>12</sup> For X-H + •Y → X• + H-Y, the TS can be described by canonical forms **I-III** and by **IV**.



The energy of the TS, *E*<sup>‡</sup>, is calculated with the requirement that the strength of the bonds being broken and being made be equal at the TS, that is, <sup>1</sup>*E*(X-H)<sup>‡</sup> = <sup>1</sup>*E*(H-Y)<sup>‡</sup>, for maximum resonance, as also suggested by Polanyi.<sup>13</sup> Therefore, bonding in **I** and **II** is required to be equal, and their average is <sup>1</sup>*E*(X-H)<sup>‡</sup>. Structure **III** gives rise to triplet repulsion, <sup>3</sup>*E*(X-Y)<sup>‡</sup>, because the electron spins at the TS must be either X↑H↓Y↑ or X↓H↑Y↓ for simultaneous partial bonding of H to both X and Y, resulting in parallel spins (triplet) on X and Y. Low BDE(X-Y) generally leads to low triplet repulsion and a lower energy. The contribution of structure **IV** is resonance stabilization from the delocalization of one electron over three atoms, *E*<sub>R</sub>, and is approximated as a constant, -10.6 kcal mol<sup>-1</sup> when X or Y is from the first two rows of the periodic table, or -12.0 kcal mol<sup>-1</sup> for X or Y beyond fluorine. The difference in BDE(RCH<sub>2</sub>-H) between propane and propene is approximately 10.6 kcal mol<sup>-1</sup>, with the odd electron delocalized over three atoms in the allyl radical. Values of the overlap integral for p orbitals of the third and higher rows justify greater resonance stabilization, *E*<sub>R</sub> = -12.0 kcal mol<sup>-1</sup>, for atoms beyond fluorine.<sup>12</sup> The energy of the TS is given by eq 6. For any stretched

$$E^\ddagger = {}^1E(X-H)^\ddagger + {}^3E(X-Y)^\ddagger + E_R \quad (6)$$

*r*(X-H) there is a corresponding *r*(H-Y) that meets the equibonding requirement and a corresponding *r*(X-Y) = *r*(X-H) + *r*(H-Y) for a linear TS. The most stable such combination of distances is the TS. An approximate zero point energy (ZPE) correction is made by assuming that ZPE<sup>‡</sup> = 1/2[ZPE(X-H) + ZPE(H-Y)]. The enthalpy of activation is given by eq 7.

(10) Heitler, W.; London, F. Z. Physik **1927**, *44*, 455.

(11) London, F. Z. Physik **1928**, *46*, 455. London, F. *Probleme der modernen Physik*, Sommerfeld Festschrift; S. Hirtzel: Leipzig, 1928.

(12) Zavitsas, A. A.; Chatgililoglu, C. J. Am. Chem. Soc. **1995**, *117*, 10645 and prior work cited therein.

(13) Polanyi, J. C. J. Chem. Phys. **1959**, *31*, 1338.

$$E^* = E^\ddagger + \text{BDE}(X-H) + \Delta(\text{ZPE}) \quad (7)$$

The relationship between our independently derived eq 6 and the London equation is more clearly seen by comparison with eq 5, rather than with eq 4. By definition, <sup>1</sup>*E*(X-H)<sup>‡</sup> is (*A* + *α*) and <sup>3</sup>*E*(X-Y)<sup>‡</sup> is (*C* - *γ*), the triplet repulsion between the terminal groups X and Y. *E*<sub>R</sub> of eq 6 corresponds to *A* of eq 5 and also accounts for the neglect of the overlap integral in the London equation. Thus, the importance of triplet repulsion for a reaction involving three electrons in a simultaneous bond-breaking and bond-making process was imbedded in the first satisfactory quantum mechanical treatment of a chemical reaction.

The Morse function,<sup>14</sup> eq 8, is used to estimate bonding at various stretched *r*(X-H) and to obtain the *r*(H-Y) that satisfies the equibonding requirement. *D*<sub>e</sub> = BDE + 0.00143*v*, where BDE is in kcal

$${}^1E = D_e(e^{-2ax} - 2e^{-ax}) \quad (8)$$

mol<sup>-1</sup> and *v* is the observed IR stretching frequency<sup>15</sup> of the bond in cm<sup>-1</sup>; *x* = *r* - *r*<sub>e</sub>, where *r* is the stretched bond length and *r*<sub>e</sub> the equilibrium bond length in angstroms; and *a* = 0.00651*ω*(*μ*/BDE)<sup>1/2</sup>. The equilibrium vibrational frequency *ω* = *v* + 0.000143*v*<sup>2</sup>/BDE and *μ* is the reduced mass in amu. The corresponding <sup>3</sup>*E*(X-Y) is estimated by the anti-Morse (or triplet repulsion) function of Sato,<sup>16</sup> eq 9, where

$${}^3E = fD_e(e^{-2ax} + 2e^{-ax}) \quad (9)$$

the original value of *f* = 0.50 was decreased to 0.45 for better agreement with ab initio results at TS distances.<sup>12</sup> The following properties of X-H, H-Y, and X-Y are needed as input data for the calculation of *E*<sup>\*</sup>: BDE, bond length, uncoupled IR stretching frequency, and masses of the bonded atoms. Therefore, calculation of *E*<sup>\*</sup> does not depend on any information derived from kinetic measurements, but only on properties of bonds in the three stable molecules. The procedure can be described a priori. The calculation has been shown to give values of *E*<sup>\*</sup> within 1 kcal mol<sup>-1</sup> of experimental Arrhenius energies of activation, *E*<sub>a</sub>, or occasionally reported enthalpies of activation, Δ*H*<sup>‡</sup>, near room temperature for over 120 hydrogen abstractions in the gas phase and in solution involving radicals on hydrogen, carbon, nitrogen, oxygen, silicon, sulfur, bromine, iodine, tin, germanium, etc.<sup>12</sup> However, for abstractions from methane by chlorine, fluorine, and hydroxyl radicals, calculated values can be as much as 3 kcal mol<sup>-1</sup> too high relative to experiment near 300 K. Because of the uncertainty of ±1 kcal mol<sup>-1</sup> in the calculation of *E*<sup>\*</sup>, we had not distinguished previously between *E*<sub>a</sub> and Δ*H*<sup>‡</sup> in comparisons with experiment.

We find that experimentally determined effects of temperature on rate constants are described by eq 10, which is equivalent to Eyring's

$$k^* = BT e^{-E^*/(RT)} \quad (10)$$

eq 3, with *B* = *κ*(*k*<sub>B</sub>/*h*) e<sup>Δ*S*<sup>‡</sup>/*R*</sup>. This work sets *B* to be a constant independent of temperature, equivalent to setting Δ*S*<sup>‡</sup> and *κ* constant. Our calculated rate constant is *k*<sup>\*</sup>. *B* relates *E*<sup>\*</sup> to the experimental rate constant, *k*<sub>exp</sub>, at a single temperature, where values of *k*<sub>exp</sub> from different sources are in good agreement: *B* = (*k*<sub>exp</sub>/*T*)e<sup>*E*<sup>\*</sup>/*RT*</sup>. *E*<sup>\*</sup> varies with temperature, as a result of variations in BDE(X-H), BDE(H-Y), and BDE(X-Y), with the other bond properties left unchanged in the calculation. With *E*<sup>\*</sup> related to experiment at one temperature, eq 10 tracks observed curvatures in plots of ln(*k*) vs 1/*T* quite well over wide temperature ranges. Equally as important, experimental data

(14) Morse, R. M. Phys. Rev. **1929**, *34*, 57. The Morse function has shortcomings (Zavitsas, A. A. J. Am. Chem. Soc. **1991**, *113*, 4755), but there is evidently sufficient cancellation of errors in calculating *E*<sup>\*</sup>. The TS distances obtained by this calculation are generally shorter than those resulting from ab initio approaches.

(15) The frequency must be uncoupled to other vibrations or should be obtained from the force constant derived from normal coordinate analysis of the IR spectrum.

(16) Sato, S. J. Chem. Phys. **1955**, *23*, 592.

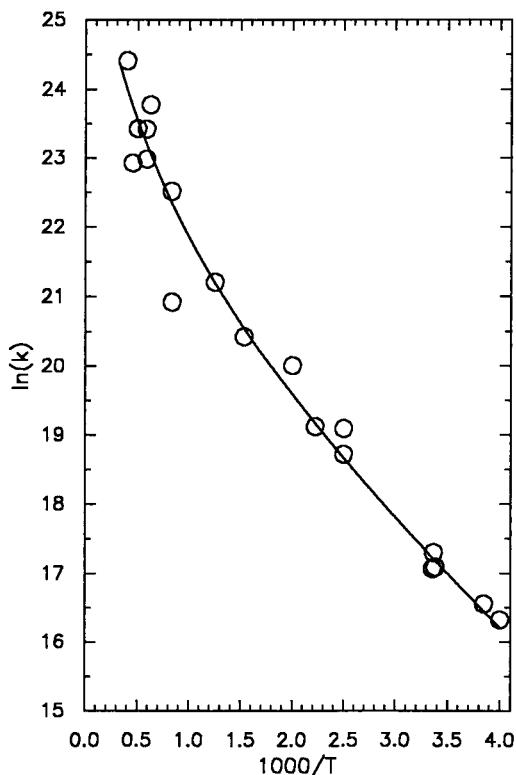


**Figure 1.** OCH-H +  $\cdot$ H. Points are experimental from 11 studies. The line is  $\ln(k^*)$  from eq 10, with  $B = 2.10 \times 10^7 \text{ L mol}^{-1} \text{ s}^{-1}$ .

showing little or no curvature are also described well. Results for typical and well-studied reactions are given below.

## Results

Reactions of formaldehyde are important in combustion, and for OCH-H +  $\cdot$ H  $\rightarrow$  OCH $\cdot$  + H-H, there are extensive rate measurements covering the broad range of 250–2500 K. Curvature in  $\ln(k)$  vs  $1/T$  plots is evident. Reviews have variously recommended  $k = (2.19 \times 10^5)T^{1.77} e^{-3.00/(RT)} \text{ L mol}^{-1} \text{ s}^{-1}$  from 300 to 2500 K,<sup>17</sup>  $k = (2.29 \times 10^7)T^{1.05} e^{-3.28/(RT)}$  from 300 to 2200 K,<sup>18</sup>  $k = (2.5 \times 10^{10}) e^{-3.99/(RT)}$  from 300 to 2500 K,<sup>19</sup> and  $k = (1.27 \times 10^7)T^{1.62} e^{-2.17/(RT)}$  from 300 to 1700 K.<sup>20</sup> Figure 1 shows the experimental results with the two extreme temperatures reported shown in each case.<sup>21</sup> The line represents  $\ln(k^*)$  from eq 10. For this reaction  $B = 2.10 \times 10^7 \text{ L mol}^{-1} \text{ s}^{-1}$  was obtained from the calculated  $E^* = 3.16 \text{ kcal mol}^{-1}$  and experimental  $k = (3.14 \pm 0.54) \times 10^7$  at 300 K,<sup>22</sup> where there is fair agreement among six experimental reports. “Anchored” at 300 K, the calculated  $\ln(k^*)$  line tracks the curvature of the data well for 2200 K, up to 2500 K.  $E^*$  increases from 3.16 kcal mol $^{-1}$  at 300 K to 3.82 at 1200 K and then slowly decreases to 3.40 at 2500 K. Although the maximum increase

of  $E^*$  here is only 0.66, this is a significant change of 21%. Table 1 shows the values of  $E^*$ ,  $\Delta H$  and,  ${}^3E$  at selected temperatures. The increase in  $E^*$  in the region of 300–1200 K is due to the combined effects of increasing triplet repulsion ( ${}^3E_{1200} - {}^3E_{300} = 0.60$ ) and decreasing exothermicity ( $\Delta\Delta H_{\text{rxn}} = +0.11$ ). The decrease of 0.42 in  $E^*$  from 1200 to 2500 K is due to decreasing  ${}^3E$  ( ${}^3E_{2500} - {}^3E_{1200} = -0.36$ ), accompanied by increasing exothermicity ( $\Delta\Delta H_{\text{rxn}} = -2.19$ ).

For the reaction  $\text{CH}_3\text{-H} + \cdot\text{H} \rightarrow \text{CH}_3\cdot + \text{H-H}$ , there are rate measurements covering the range from 378 to 2300 K. Curvature of  $\ln(k)$  vs  $1/T$  plots is evident, and reviews have fitted the data variously by  $k = 22.5T^{3.00} e^{-8.76/(RT)} \text{ L mol}^{-1} \text{ s}^{-1}$  over the range 300–2500 K,<sup>17</sup>  $k = 13.3T^{3.00} e^{-8.04/(RT)}$  over the same range,<sup>18</sup> or  $k = (3.86 \times 10^3)T^{2.11} e^{-7.75/(RT)}$  over 400–1800 K.<sup>19</sup> Figure 2 shows experimental results from 14 different sources.<sup>19</sup> There is good agreement between three recent reviews at 1000 K where  $k = (2.59 \pm 0.39) \times 10^8$ , from which  $B = 1.31 \times 10^8$  with  $E^* = 12.36$ . The line in Figure 2 is  $\ln(k^*)$  from eq 10. The experimental curvature is described well. Table 1 shows that  $E^*$  increases by 1.14 kcal mol $^{-1}$  (from 11.22 to 12.36) in going from 300 to 1000 K, while  $\Delta H_{\text{rxn}}$  increases by 0.63 (from 0.61 to 1.23) and  ${}^3E$  increases by 0.62 (from 16.87 to 17.49). Thus, the increase in  $E^*$  in this region is due to the combined effects of increasing endothermicity and increasing X–Y triplet repulsion.  $E^*$ ,  ${}^3E$ , and  $\Delta H_{\text{rxn}}$  do not rise monotonically.  $E^*$  reaches its maximum value of 12.37 at 1200 K and then declines to 11.45 at 2500 K. A curved plot at high temperatures, despite decreasing  $E^*$  in that region, is caused by the linear dependence of the rate constant on  $T$ , eq 10.  ${}^3E$  rises to a maximum of 17.63 at 1500–1700 K and then declines to 17.47 at 2500 K, because BDE(X–Y) starts declining above 2000 K. The reaction is endothermic at 300 K but becomes exothermic at 1900 K and  $\Delta H_{\text{rxn}} = -1.19$  at 2500 K, a change of  $-2.51 \text{ kcal mol}^{-1}$  from 800 K.

For the reaction  $\text{H-H} + \cdot\text{CH}_3 \rightarrow \text{H}\cdot + \text{H-CH}_3$ , there are fewer and more scattered measurements compared to its reverse. Reviews have described the data by  $k = 0.289T^{3.12} e^{-8.71/(RT)}$  for 300 K to 2500 K,<sup>17</sup>  $k = 6.87T^{2.74} e^{-9.42/(RT)}$  for the same range,<sup>18</sup> or  $k = 39.8T^{2.24} e^{-6.40/(RT)}$  for 400–1800 K.<sup>19</sup> There is fair agreement at 1500 K between two measurements and four recent reviews,<sup>17–19</sup>  $k = (1.23 \pm 0.37) \times 10^8$ , from which  $B = 4.17 \times 10^6$  with  $E^* = 11.66$ . Figure 3 shows the existing data from six different reports between 372 and 2320 K;<sup>19</sup> the solid line is  $\ln(k^*)$  from eq 10 and is consistent with the data. Table 1 shows that, unlike its reverse reaction, the calculated enthalpy of activation here increases monotonically, even though the reaction is becoming increasingly exothermic between 300 and 1000 K;  $\Delta H_{\text{rxn}}$  goes from  $-0.61$  at 300 K to  $-1.23$  at 1000 K. Despite this, the reaction at 1000 K has a higher  $E^*$  by 0.52 because of an increase of 0.62 in  ${}^3E$ .

Figure 3 is less curved than Figure 2 below 800 K and more curved above. This can be understood as follows. For a reaction and its reverse, the effect of changes in  $\Delta H_{\text{rxn}}$  will be in opposite directions. Triplet repulsion is common to both reactions, and here  ${}^3E$  increases from 300 to 2000 K then declines slightly.  $\Delta H_{\text{rxn}}(\text{H-H} + \cdot\text{CH}_3)$  is becoming more exothermic between 300 and 800 K, thus counterbalancing the effect of increasing  ${}^3E$  on  $E^*$ . The enthalpy of activation increases by only 0.33 kcal mol $^{-1}$ . For the reverse reaction,  $\Delta H_{\text{rxn}}(\text{CH}_3\text{-H} + \cdot\text{H})$  is becoming more endothermic and this adds to the effect of increasing  ${}^3E$ . Thus,  $E^*$  for  $\text{CH}_3\text{-H} + \cdot\text{H}$  increases by 1.19, producing greater curvature in Figure 2 than in Figure 3 in the 300–800 K region. The opposite occurs in the 1000–2500 K region.  $\Delta H_{\text{rxn}}(\text{H-H} + \cdot\text{CH}_3)$  becomes more

(17) Tsang, W.; Hampson, R. F. *J. Phys. Chem. Ref. Data* **1986**, *15*, 108.

(18) Baulch, D. L.; Cobos, C. J.; Cox, R. A.; Esser, C.; Frank, P.; Just, Th.; Kerr, J. A.; Pilling, M. J.; Troe, J.; Walker, R. W.; Warnatz, J. *J. Phys. Chem. Ref. Data* **1992**, *21*, 411.

(19) Mallard, W. G.; Westley, F.; Herron, J. T.; Hampson, R. F.; Frizzell, D. H. *NIST Chemical Kinetics Database: Version 6.0*; National Institute of Standards and Technology: Gaithersburg, MD, 1994.

(20) Baulch, D. L.; Cobos, C. J.; Cox, R. A.; Frank, P.; Hayman, G.; Just, Th.; Kerr, J. A.; Murrells, T.; Pilling, M. J.; Troe, J.; Walker, R. W.; Warnatz, J. *J. Phys. Chem. Ref. Data* **1994**, *23*, 847.

(21) A point in the middle of the range is plotted occasionally in this and subsequent figures when a wide gap would otherwise appear in the plots. Measurements are as cited in refs 17–19, unless otherwise indicated.

(22) Rate constants are expressed in  $\text{L mol}^{-1} \text{ s}^{-1}$  throughout, and energies are in kcal mol $^{-1}$ .

**Table 1.** Values of  $E^*$ ,  $\Delta H_{\text{rxn}}$  and  ${}^3E$  (kcal mol $^{-1}$ ) at Selected Temperatures

	T, K								
	300	400	500	600	800	1000	1500	2000	2500
OCH-H + $\cdot\text{H}$									
$E^*$	3.16	3.33	3.46	3.58	3.73	3.80	3.77	3.61	3.40
$\Delta H_{\text{rxn}}$	-14.91	-14.74	-14.63	-14.58	-14.60	-14.77	-15.49	-16.36	-17.22
${}^3E$	11.82	11.96	12.06	12.17	12.33	12.40	12.38	12.28	12.06
CH $_3$ -H + $\cdot\text{H}$									
$E^*$	11.22	11.52	11.79	11.99	12.26	12.36	12.23	11.78	11.45
$\Delta H_{\text{rxn}}$	0.61	0.87	1.08	1.22	1.32	1.23	0.57	-0.30	-1.19
${}^3E$	16.87	17.04	17.18	17.25	17.38	17.49	17.63	17.47	17.47
H-H + $\cdot\text{CH}_3^a$									
$E^*$	10.61	10.65	10.71	10.77	10.94	11.13	11.66	12.17	12.64
$\Delta H_{\text{rxn}}$	-0.61	-0.87	-1.08	-1.22	-1.32	-1.23	-0.57	0.30	1.19
C $_2$ H $_5$ -H + $\cdot\text{CH}_3$									
$E^*$	12.11	12.59	12.59	12.15	12.03	11.86	11.08		
$\Delta H_{\text{rxn}}$	-4.31	-4.45	-4.59	-4.69	-4.87	-4.98	-5.93		
${}^3E$	18.88	19.36	19.34	19.05	19.05	18.87	18.45		
C $_2$ H $_5$ -H + $\cdot\text{H}$									
$E^*$	8.47	8.64	8.77	8.91	9.03	9.07	8.90	8.57	8.21
$\Delta H_{\text{rxn}}$	-3.70	-3.58	-3.55	-3.47	-3.55	-3.75	-4.56	-5.51	-6.42
${}^3E$	15.67	15.85	15.98	16.00	16.13	16.17	16.10	15.98	15.81
H-H + $\cdot\text{C}_2\text{H}_5^b$									
$E^*$	12.17	12.22	12.32	12.38	12.58	12.82	13.46		
$\Delta H_{\text{rxn}}$	3.70	3.58	3.55	3.47	3.55	3.75	4.56		
CH $_3$ -H + $\cdot\text{Br}$									
$E^*$	18.73	19.05	19.29	19.47	19.66	19.69	19.34		
$\Delta H_{\text{rxn}}$	17.28	17.53	17.75	17.89	18.02	18.01	17.51		
${}^3E$	11.97	12.03	12.07	12.10	12.16	12.13	12.28		
H-H + $\cdot\text{Br}$									
$E^*$	19.04	19.12	19.22	19.31	19.49	19.68	20.13	20.45	20.66
$\Delta H_{\text{rxn}}$	16.67	16.66	16.67	16.67	16.70	16.78	16.94	16.99	16.93
${}^3E$	12.28	12.31	12.39	12.29	12.57	12.69	12.92	13.19	13.38
H-H + $\cdot\text{OH}$									
$E^*$	3.53	3.61	3.68	3.74	3.88	4.02	4.34	4.58	4.78
$\Delta H_{\text{rxn}}$	-15.01	-15.11	-15.19	-15.25	-15.29	-15.26	-15.01	-14.67	-14.31
${}^3E$	13.18	13.26	13.33	13.40	13.54	13.68	13.98	14.23	14.43

<sup>a</sup>  ${}^3E$  is common with the reaction CH $_3$ -H +  $\cdot\text{H}$ . <sup>b</sup>  ${}^3E$  is common with the reaction C $_2$ H $_5$ -H +  $\cdot\text{H}$ .

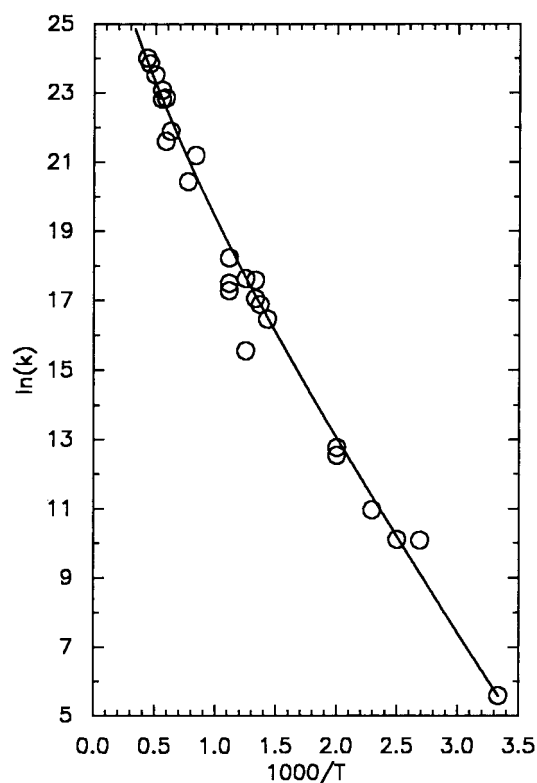


**Figure 2.** CH $_3$ -H +  $\cdot\text{H}$ . Points are experimental from 14 studies. The line is  $\ln(k^*)$  from eq 10, with  $B = 1.31 \times 10^8 \text{ L mol}^{-1} \text{ s}^{-1}$ .

positive by 2.42 and contributes to an increase of 1.51 in  $E^*$ . For the reverse reaction in the same temperature range,  $\Delta H_{\text{rxn}}$ -(CH $_3$ -H +  $\cdot\text{H}$ ) becomes more negative by 2.42 and counterbalances the effect of  ${}^3E$ . The result is a decrease of 0.91 in  $E^*$

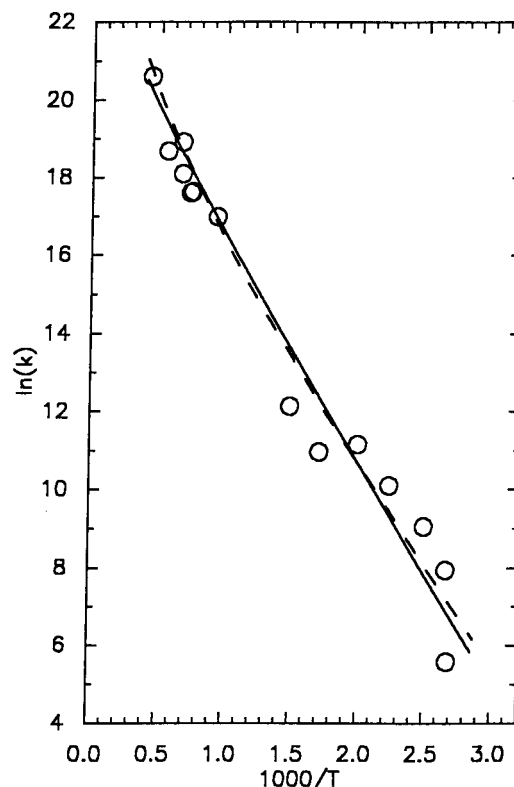


**Figure 3.** H-H +  $\cdot\text{CH}_3$ . Points are experimental from six studies. The solid line is  $\ln(k^*)$  from eq 10, with  $B = 4.17 \times 10^6 \text{ L mol}^{-1} \text{ s}^{-1}$ . The dashed line is obtained from  $k^*(\text{CH}_3\text{-H} + \cdot\text{H})$  divided by the thermodynamic equilibrium constant for  $\text{CH}_3\text{-H} + \cdot\text{H} \rightleftharpoons \text{CH}_3\cdot + \text{H-H}$  between 1000 and 2500 K and a less curved plot in Figure 2, compared to the same region in Figure 3.

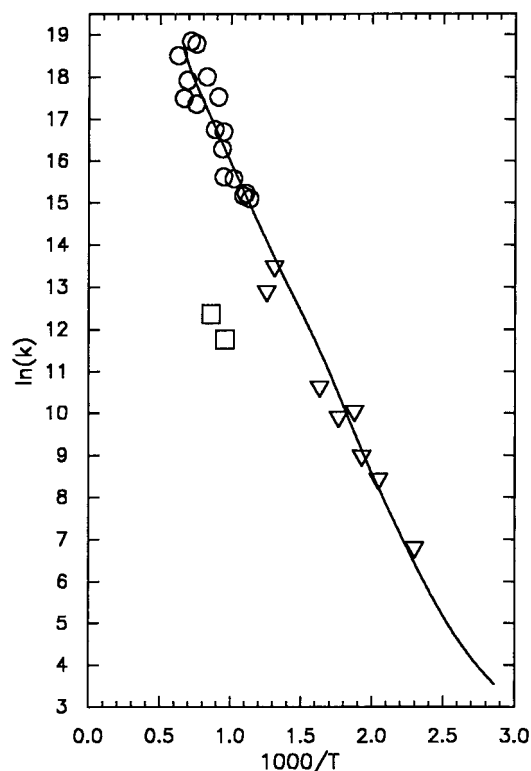


**Figure 4.**  $\text{CH}_3\text{CH}_2\text{-H} + \bullet\text{CH}_3$ . Points are experimental from 13 studies, with inverted triangles pertaining to abstraction by  $\bullet\text{CD}_3$ . The line is  $\ln(k^*)$  from eq 10, with  $B = 3.35 \times 10^6 \text{ L mol}^{-1} \text{ s}^{-1}$ .

For the reaction  $\text{CH}_3\text{CH}_2\text{-H} + \bullet\text{CH}_3 \rightarrow \text{CH}_3\text{CH}_2\bullet + \text{H-CH}_3$ , rate measurements below 800 K pertain to abstractions by  $\bullet\text{CD}_3$ .<sup>18</sup> Reviews have recommended  $k = 0.00054T^{4.00} e^{-8.29/(RT)}$  for 300–2500 K<sup>17</sup> or  $k = (1.51 \times 10^{-10})T^{6.00} e^{-6.05/(RT)}$  for 300–1500 K.<sup>18</sup> Figure 4 shows experimental values from 13 different sources<sup>19</sup> and distinguishes between  $\bullet\text{CH}_3$  and  $\bullet\text{CD}_3$  results.<sup>23</sup> There is fair agreement for the rate constants reported in the region of 900–1000 K, from which we obtain  $B = 3.35 \times 10^6$ . Figure 4 shows that experimental values are tracked well by the line of calculated  $\ln(k^*)$ , which shows pronounced curvature in the 300–600 K region but minimal curvature above 600 K. This is consistent with the fact that all but one of the experimental studies above 980 K have reported linear  $\ln(k)$  vs  $1/T$  behavior. If one set of data, shown by open squares in Figure 4, is disregarded as being much too far from the consensus, the best three-parameter fit of the available<sup>19</sup> points in the region of 920–2100 K is  $k = (7.21 \times 10^8)T^{0.39} e^{-14.70/(RT)}$ , which is very nearly a straight line. The curvature in the lower temperature region is due to an increasing value of  $E^*$  caused by increasing triplet repulsion, even though the reaction is becoming slightly more exothermic (Table 1). From 500 to 1500 K,  $E^*$  decreases by 1.51, a result of the combined effects of a corresponding increase in exothermicity of  $\Delta\Delta H_{\text{rxn}} = -1.34$  and a decrease in X–Y triplet repulsion of  $\Delta^3E = -0.91$ , the latter due to decreasing  $\text{BDE}(\text{CH}_3\text{CH}_2\text{-CH}_3)$  in this region. This decrease in  $E^*$  above 500 K nearly counterbalances the curvature normally produced by the linear dependence of  $k$  on  $T$ , eq 10. Thermodynamic data are not available for calculating  $\text{BDE}(\text{C}_2\text{H}_5\text{-CH}_3)$  and, therefore,  $E^*$  above 1500 K.

(23) The two earliest reports (1939 and 1951) have been omitted. The 1955 results of McNesby and Gordon (quoted in ref 18) have also been omitted and have been replaced by two later results: McNesby, J. R. *J. Phys. Chem.* **1960**, *64*, 1671. Jackson, W. M.; McNesby, J. R.; Darwent, B. de B. *J. Chem. Phys.* **1962**, *37*, 1610.

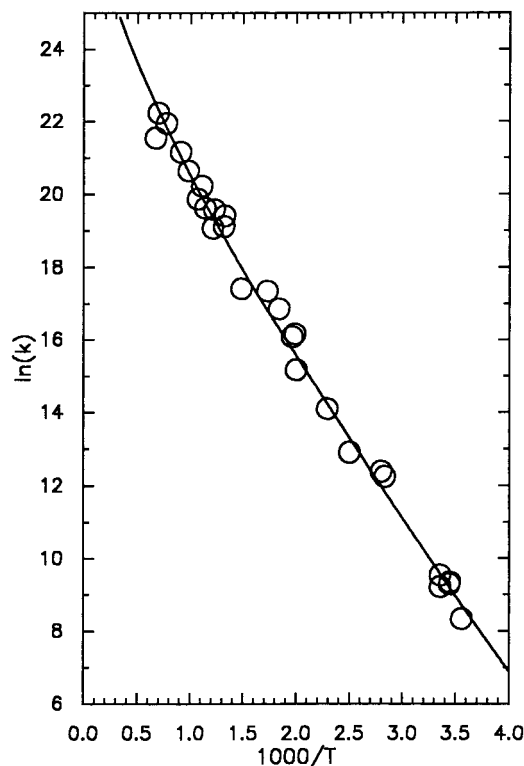


**Figure 5.**  $\text{CH}_3\text{CH}_2\text{-H} + \bullet\text{H}$ . Points are experimental from 15 studies. The line is  $\ln(k^*)$  from eq 10, with  $B = 7.90 \times 10^7 \text{ L mol}^{-1} \text{ s}^{-1}$ .

For the reaction  $\text{CH}_3\text{CH}_2\text{-H} + \bullet\text{H} \rightarrow \text{CH}_3\text{CH}_2\bullet + \text{H-H}$ , there are experimental measurements in the range of 281–1485 K from 15 different sources.<sup>17–19</sup> Reviews have recommended  $k = 0.554T^{3.50} e^{-5.17/(RT)}$  for 300–2500 K,<sup>17</sup>  $k = (1.44 \times 10^6)T^{1.50} e^{-7.41/(RT)}$  for 300–2000 K,<sup>18</sup> or  $k = (1 \times 10^{11}) e^{-9.60/(RT)}$  for 300–2000 K.<sup>19</sup> There is fair agreement between the various sources at 300 K where  $k = (1.60 \pm 0.31) \times 10^4$ , from which we obtain  $B = 7.90 \times 10^7$  with  $E^* = 8.47$ . Figure 5 shows the experimental data,<sup>19</sup> and the line is  $\ln(k^*)$  from eq 10. “Anchored” at 300 K, the calculated line tracks the experimental curvature well over a range of 1200 K. Table 1 shows that  $\Delta H_{\text{rxn}}$  changes little between 300 and 1000 K, but  $E^*$  increases by 0.60 kcal mol<sup>-1</sup> because of increasing triplet repulsion,  $\Delta^3E = 0.50$ . Between 1000 and 2500 K, triplet repulsion decreases ( ${}^3E_{2500} - {}^3E_{1000} = -0.86$ ), the exothermicity of the reaction increases ( $\Delta\Delta H_{\text{rxn}} = -2.67$ ), and the result is a decrease in  $E^*$ ,  $\Delta E^* = -0.86$ . To some extent this decrease counteracts the curvature produced by the linear dependence of  $k$  on  $T$ , eq 10.

For the reaction  $\text{H-H} + \bullet\text{CH}_2\text{CH}_3 \rightarrow \text{H}\bullet + \text{H-CH}_2\text{CH}_3$ , there are four experimental reports covering the range from 513 to 1200 K and two estimates.<sup>19</sup> A recommendation<sup>20</sup> from 700 to 1200 K is  $k = 0.00308T^{3.6} e^{-8.24/(RT)}$ . From the best fits to experimental points and the two estimates,  $k = (1.74 \pm 0.61) \times 10^6$  at 1000 K, from which  $B = 1.1 \times 10^6$  with  $E^* = 12.82$ . The calculated  $\ln(k^*)$  is shown as the solid line in Figure 6. Agreement with existing measurements is acceptable. From 300 to 1500 K,  $\Delta H_{\text{rxn}}$  increases by 0.86 and  ${}^3E$  increases by 0.43, resulting in an increase of 1.29 in  $E^*$  (Table 1). The increase in  $E^*$  is monotonic for this reaction, unlike its reverse reaction above.

For the reaction  $\text{CH}_3\text{-H} + \bullet\text{Br} \rightarrow \text{CH}_3\bullet + \text{H-Br}$ , there are five experimental reports compiled,<sup>19</sup> and we added Kistiakowsky’s classic 1944 study that established  $\text{BDE}(\text{CH}_3\text{-H})$  on a sound basis.<sup>24</sup> The measurements cover the range 419–704

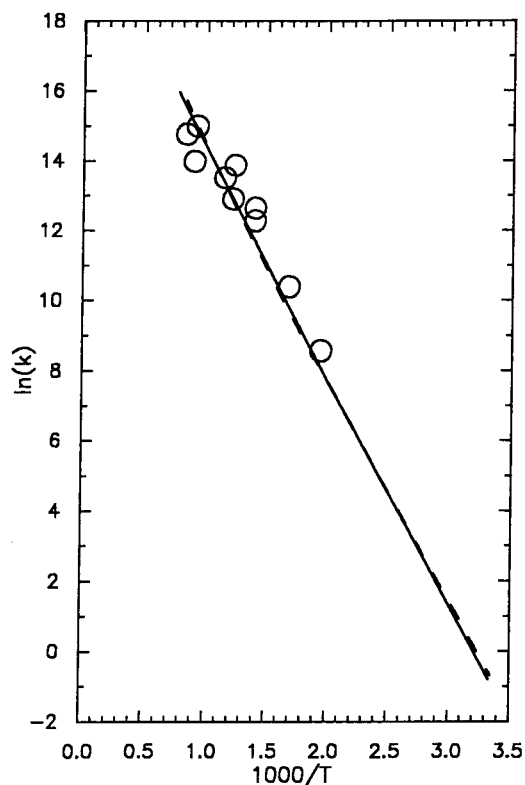


**Figure 6.** H-H +  $\cdot\text{CH}_2\text{CH}_3$ . Points are experimental from four studies. The solid line is  $\ln(k^*)$  from eq 10, with  $B = 1.1 \times 10^6 \text{ L mol}^{-1} \text{ s}^{-1}$ . The dashed line is obtained from  $k^*(\text{CH}_3\text{CH}_2\text{-H} + \cdot\text{H})$  divided by the thermodynamic equilibrium constant for  $\text{CH}_3\text{CH}_2\text{-H} + \cdot\text{H} \rightleftharpoons \text{CH}_3\text{CH}_2\cdot + \text{H-H}$ .

K, and no curved plots have been reported, perhaps because of the limited temperature range. Measured rate constants in the vicinity of 500 K give  $k = (6.46 \pm 2.04) \times 10^2$ , from which we obtain  $B = 3.5 \times 10^8$  with  $E^* = 19.29$ . With this value of  $B$ ,  $\ln(k^*)$  from eq 10 is shown as the line in Figure 7. Agreement is excellent with all but one of the sets of data. The increase in  $E^*$  is not monotonic (Table 1).  $\Delta H_{\text{rxn}}$  and  ${}^3E$  change relatively little, leading to a small percent change in  $E^*$  ( $E^*_{1500} - E^*_{300} = 0.57$ ), and there is only a small curvature in Figure 7 in the temperature domain for which measurements exist.

For the reaction  $\text{H-H} + \cdot\text{Br} \rightarrow \text{H}\cdot + \text{H-Br}$ , experimental data have been compiled from six sources.<sup>19</sup> We added the pioneering 1906 study of Bodenstein<sup>25</sup> and data from three more sources.<sup>26</sup> The data extend to 1700 K. Curvature either is not reported or is small, for example, from the most recent review  $k = (4.16 \times 10^9)T^{0.43} e^{-17.83/(RT)}$  for the range 214–1700 K.<sup>19</sup> Four reviews give  $k = (7.81 \pm 1.13) \times 10^2$  at 500 K,<sup>19</sup> from which  $B = 3.3 \times 10^8$  with  $E^* = 19.22$ . With this value of  $B$ ,  $\ln(k^*)$  from eq 10 is shown as the line in Figure 8, along with the experimental points.  $\Delta H_{\text{rxn}}$  is almost invariant, and  ${}^3E$  increases by only 0.75 from 300 to 1700 K (Table 1), consistent with the lack of pronounced curvature in the experimental data. Close examination of Figure 8 indicates that  $E^*$  may be slightly high, but it should be noted that the experimental rate constants are being tracked by the calculated  $k^*$  over a range of 12 powers of 10.

(24) Kistiakowsky, G. B.; Van Artsdalen, R. E. *J. Chem. Phys.* **1944**, *12*, 469.

(25) Bodenstein, M.; Lind, S. C. *Z. Phys. Chem.* **1906**, *57*, 168.

(26) Bach, F.; Bonhoeffer, K. F.; Moelwyn-Hughes, E. A. *Z. Phys. Chem. Abt. B*, **1935**, *27*, 71. Fettis, G. C.; Knox, J. H.; Trotman-Dickenson, A. F. *J. Chem. Soc.* **1960**, 4177. Skinner, G. B.; Ringrose, G. H. *J. Chem. Phys.* **1965**, *43*, 4129.

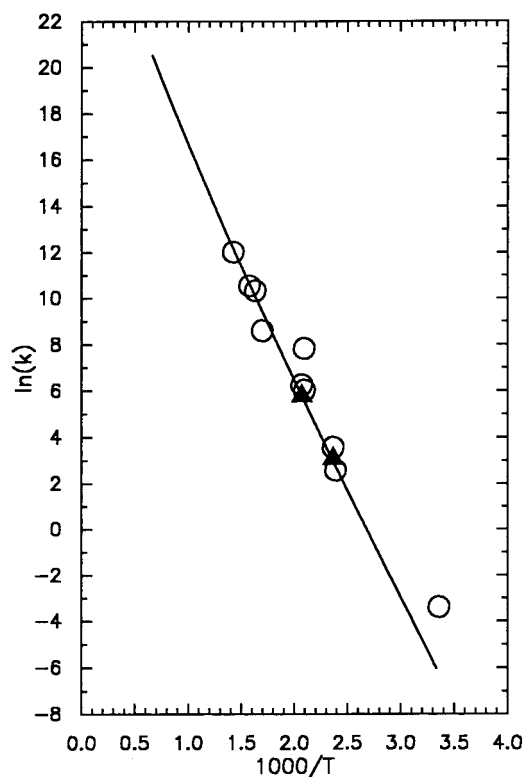


**Figure 7.**  $\text{CH}_3\text{-H} + \cdot\text{Br}$ . Points are experimental from six studies. The line is  $\ln(k^*)$  from eq 10, with  $B = 3.5 \times 10^8 \text{ L mol}^{-1} \text{ s}^{-1}$ . The filled triangles are from ref 24.

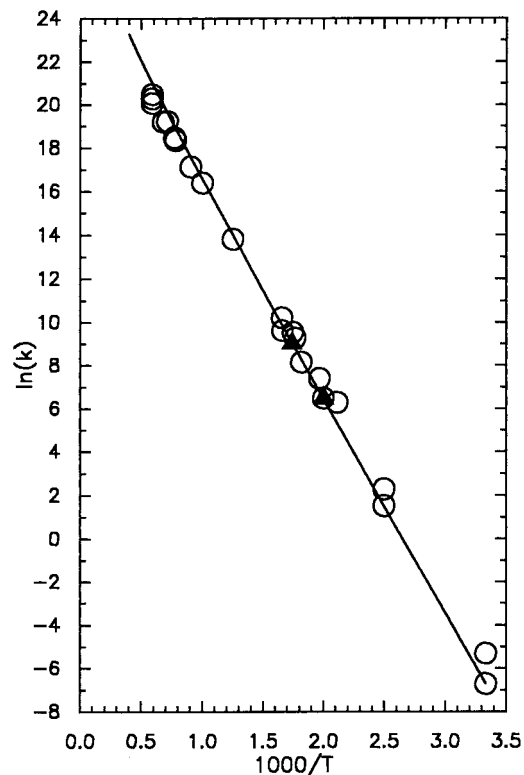


**Figure 8.** H-H +  $\cdot\text{Br}$ . Points are experimental from 10 studies. The line is  $\ln(k^*)$  from eq 10, with  $B = 3.1 \times 10^8 \text{ L mol}^{-1} \text{ s}^{-1}$ . The filled triangles are from ref 25.

The reactions treated above met three necessary criteria: (a) thermodynamic functions were available in standard databases for obtaining BDE values over wide temperature ranges and the other molecular data needed for calculating  $E^*$  were reliable;

**Table 2.** Changes in Energy of Activation with Temperature.<sup>a</sup>

reaction	$E_a^*(300\text{ K})^b$	$E_a^*(1500\text{ K})^b$	$\Delta E_a^*^c$
OCH-H + •H	3.8	6.8	3.0
CH <sub>3</sub> -H + •H	11.8	15.2	3.4
H-H + •CH <sub>3</sub>	11.2	14.6	3.4
C <sub>2</sub> H <sub>5</sub> -H + •CH <sub>3</sub>	12.7	14.1	1.3
C <sub>2</sub> H <sub>5</sub> -H + •H	9.1	11.9	2.8
H-H + •C <sub>2</sub> H <sub>5</sub>	12.8	16.4	3.7
CH <sub>3</sub> -H + •Br	19.3	22.3	3.0
H-H + •Br	19.7	23.2	3.5
H-H + •OH	4.1	7.3	3.2
H-H + •OH	4.4 <sup>d</sup>	7.7 <sup>d</sup>	3.3 <sup>d</sup>

<sup>a</sup> Values in kcal mol<sup>-1</sup>.  $RT = 0.6$  at 300 K and 3.0 at 1500 K;  $\Delta(RT) = 2.4$ . <sup>b</sup>  $E_a^* = E^* + RT$ . <sup>c</sup>  $\Delta E_a^* = E_a^*(1500\text{ K}) - E_a^*(300\text{ K})$ .

<sup>d</sup> Obtained from experimental data, see text.

(b) a number of different kinetic studies were available over wide temperature ranges; and (c) the calculated  $E^*$  matched very closely with experiment.

The energy of activation defined in the Arrhenius sense is  $E_a = -R[d \ln(k)/d(1/T)]$ , that is, it can be obtained from the slope of  $\ln(k)$  vs  $1/T$  at any temperature. From eq 10,  $E_a^*$  can be similarly defined as  $E^* + RT$ . Table 2 lists changes in  $E_a^*$  from 300 to 1500 K. The  $RT$  term adds 2.4 kcal mol<sup>-1</sup>, but the increase in  $E_a^*$  is different for each of the various reactions. In all but one case it is more than 2.4, but the exception demonstrates the variety of behavior that is possible. Table 2 includes the reaction  $\text{H}_2 + \bullet\text{OH}$ , which is important in combustion and has been extensively studied. However this reaction does not satisfy criterion c above, in that the  $E^*$  calculation underestimates experiment by about 0.4 kcal mol<sup>-1</sup>. While this is within the normal error of the  $E^*$  calculation, here it amounts to a significant percent of the low enthalpy of activation of this reaction and, as a result,  $\ln(k^*)$  does not rise steeply enough with temperature to match experiment well. Nevertheless, Table 2 demonstrates that the change in calculated  $E_a^*$  is consistent with experiment. The best three-parameter fit to 40 different rate studies in the range of 210–2800 K<sup>27</sup> is  $k = (3.86 \times 10^5)T^{1.42} e^{-3.45/(RT)}$ ; from the slope of experimental  $\ln(k)$  vs  $1/T$  in this case,  $E_a = 3.45 + 1.42RT$ . The values of the last line in Table 2 pertain to  $E_a$  values so obtained. It can be seen that there is agreement, within expected experimental uncertainty, between  $\Delta E_a$  from experimental information and the calculated  $\Delta E_a^*$ , 3.3 vs 3.2 kcal mol<sup>-1</sup>.

Equation 10 is equivalent to the Eyring eq 3, with  $B = \kappa(k_B/h) e^{\Delta S^\ddagger/R} = \text{constant}$ , equivalent to setting  $\Delta S^\ddagger$  and  $\kappa$  to be independent of temperature. Experimental data are fitted well by the calculated  $\ln(k^*)$  from eq 10 in Figures 1–8. However, the entropy change,  $\Delta S_{\text{rxn}}$ , for the reactions treated here is not temperature independent. For example, for  $\text{CH}_3\text{-H} + \bullet\text{H} \rightarrow \text{CH}_3\bullet + \text{H-H}$ ,  $\Delta S_{\text{rxn}}$  increases from 5.74 eu at 300 K to 7.35 eu at 800 K and then declines to 6.73 eu at 1500 K.<sup>28</sup> Similarly, for  $\text{CH}_3\text{CH}_2\text{-H} + \bullet\text{H} \rightarrow \text{CH}_3\text{CH}_2\bullet + \text{H-H}$ ,  $\Delta S_{\text{rxn}}$  is 8.09 eu at 300 K, 8.70 eu at 600 K, and 7.71 eu at 1500 K.<sup>29</sup> Such changes

(27) Forty-one sets of experimental data are compiled in ref 19. One measurement, coded 56BAL, is conspicuously too far from all other measurements. After excluding this one value, the best three-parameter fit was obtained for the remaining 40 experimental results by the built-in nonlinear fitting program of ref 19. Essentially the same expression,  $k = (2.16 \times 10^5)T^{1.51} e^{-3.43/(RT)}$ , is reported by Michael, J. V.; Sutherland, J. W. *J. Phys. Chem.* **1988**, *92*, 3853.

(28) Afeefy, H. Y.; Liebman, J. F.; Stein, S. E. *Neutral Thermochemical Data* in NIST Standard Reference Database Number 69, Mallard, W. G., Linstrom, P. J., Eds.; August 1997, National Institute of Standards and Technology: Gaithersburg, MD (<http://webbook.nist.gov>). This work provides the appropriate coefficients to the Shomate equation, and the  $\Delta H$  values obtained are essentially the same as the values the JANAF Thermochemical Tables provide for the molecules used here (Chase, M. E.; et al. *J. Phys. Chem. Ref. Data* **1985**, *14* (Suppl. 1)).

**Table 3.** Equilibrium Constants for  $\text{X-H} + \bullet\text{Y} \rightleftharpoons \text{X}\bullet + \text{H-Y}$  and Their Temperature Dependence As Calculated from  $k_1^*$  and  $k_{-1}^*$ . Given by Eq 10, from Thermodynamic Databases, and from Other Sources of  $k_1$  and  $k_{-1}$ 

temp (K)	$\log(k_1/k_{-1})^*$ (eq 10)	$\log(K_e)$ (NIST-25) <sup>a</sup>	$\log(K_e)$ (NIST-69) <sup>b</sup>	$\log(K_e)$ (NASA) <sup>c</sup>	$\log(k_1/k_{-1})$ (ref 17)	$\log(k_1/k_{-1})$ (ref 18)
Reaction: $\text{CH}_3\text{-H} + \bullet\text{H} \rightleftharpoons \text{CH}_3\bullet + \text{H-H}$						
300	1.05	0.9	0.80	0.88	1.55	1.94
400	1.02	1.0	0.94	0.80	1.55	1.72
500	1.01	1.0	1.04	0.93	1.57	1.59
600	1.05	1.1	1.13	1.03	1.56	1.51
800	1.14	1.1	1.24	1.16	1.54	1.42
1000	1.23	1.1	1.31	1.24	1.52	1.37
1500	1.41	1.2	1.39	1.31	1.51	1.31
2000	1.53		1.39	1.30	1.50	1.30
Reaction: $\text{CH}_3\text{CH}_2\text{-H} + \bullet\text{H} \rightleftharpoons \text{CH}_3\text{CH}_2\bullet + \text{H-H}$						
300	4.55	4.4	4.45 <sup>d</sup>	4.48		
400	3.81	3.7	3.51 <sup>d</sup>	3.84		
500	3.41	3.3	3.26 <sup>d</sup>	3.41		
600	3.12	3.0	3.03 <sup>d</sup>	3.17		
800	2.83	2.6	2.66 <sup>d</sup>	2.85		
1000	2.68	2.4	2.58 <sup>d</sup>	2.65		
1200	2.59		2.29 <sup>d</sup>	2.50		
1500	2.52	2.1	2.12 <sup>d</sup>	2.35		

<sup>a</sup> Estimated by the program of NIST Standard Reference Database 25.<sup>30</sup> <sup>b</sup> Calculated from the data of NIST Standard Reference Database 69.<sup>28</sup> <sup>c</sup> Calculated from the data of NASA Lewis Research Center.<sup>29</sup>

<sup>d</sup> Calculated using  $\text{H} - \text{H}_{298}$  and  $S$  values given in NIST Standard Reference Database 25 for  $\text{C}_2\text{H}_6$  and  $\text{C}_2\text{H}_5$ .

in  $\Delta S_{\text{rxn}}$  may influence the entropy of activation. For example, if it were assumed that one-half of the maximum variation in  $\Delta S_{\text{rxn}}$  would be reflected in the TS, the effect on the rate constant would be about 50% for the methane reaction with  $\bullet\text{H}$ , but only 17% for that of ethane. In addition, the methane reaction is nearly thermoneutral, and  $\Delta S_{\text{rxn}}$ , rather than  $\Delta H_{\text{rxn}}$ , is the predominant equilibrium factor at all temperatures. For the more common cases of endothermic or exothermic reactions, as with ethane here,  $\Delta H_{\text{rxn}}$  is important at lower temperatures and its influence on equilibria declines with increasing temperature. The magnitude of the effect introduced by setting  $\Delta S^\ddagger = \text{constant}$  is examined below.

Since eq 10 yields rate constants for the forward and reverse reactions independent of the thermodynamic equilibrium constant,  $K_e$ , we calculate  $K_e^* = k_1^*/k_{-1}^*$  and compare with  $K_e$  values obtainable from reported  $S$  and  $\Delta H$  values of products and reactants from standard thermodynamic databases,  $\log(K_e) = [\Delta S_{\text{rxn}}/R - \Delta H_{\text{rxn}}/(RT)]/2.303$ . This comparison is shown in Table 3. If the entropy of activation were invariant (with  $\kappa = \text{constant}$ ), there should be agreement between  $\log(K_e^*)$  and  $\log(K_e)$ , assuming that the tabulated thermodynamic functions are perfectly correct over the temperature ranges in question. With the methane reaction, there are discrepancies between columns 2 and 4, even though the BDE values used for the calculation of  $E^*$  were derived from the NIST-69 database.<sup>28</sup> In this, the more stringent test case, the average discrepancy is 0.098 log unit; for assessing this, one can compare it with the average discrepancy in  $\log(K_e)$  values of 0.094 log units obtainable from two standard thermodynamic databases (columns 4 and 5). The assumption of constant entropy of activation leads to deviations not much greater than differences in standard databases. With ethane, there should be agreement between columns 2 and 5, since the NASA values were used for BDE- $(\text{C}_2\text{H}_5\text{-H})$ . The average discrepancy between  $\log(k_1^*/k_{-1}^*) = \log(K_e^*)$  and thermodynamic  $\log(K_e)$  is only 0.056 log unit for

(29) Data provided by M. J. Rabinowitz of NASA Lewis Research Center and available on the Internet at [http://www.me.berkeley.edu/gri\\_mech/](http://www.me.berkeley.edu/gri_mech/).

**Table 4.** BDE Values Used (kcal mol<sup>-1</sup>) at Selected Temperatures and Bond Properties

T, K	H-H	OCH-H	CH <sub>3</sub> -H	C <sub>2</sub> H <sub>5</sub> -H	C <sub>2</sub> H <sub>5</sub> -CH <sub>3</sub>	H-Br	CH <sub>3</sub> -Br	H-OH
250	104.06	89.07		100.28				
300	104.21	89.30	104.82	100.51	88.91	87.54	70.93	119.23
350	104.36	89.56	105.11	100.72	88.88		70.93	
400	104.51	89.77	105.38	100.93	90.28	87.85	71.33	119.63
450	104.66	89.98	105.64					
500	104.81	90.17	105.89	101.31	90.42	88.14	71.56	120.00
600	105.10	90.52	106.32	101.63	89.43	88.43	71.77	120.35
700	105.39	90.82	106.69	101.90	89.36	88.70	71.97	120.67
800	105.68	91.08	107.00	102.13	89.32	88.98	72.01	120.97
900	105.96	91.29	107.26	102.32	89.17	89.22	72.02	121.24
1000	106.24	91.47	107.47	102.49	88.98	89.46	72.12	121.50
1100	106.50	91.62	107.64	102.61	88.75	89.69	72.07	121.73
1200	106.76	91.74	107.78	102.71	88.57	89.90	72.07	121.94
1300	107.01	91.84	107.89	102.79	88.46	90.13	72.13	122.14
1400	107.25	91.92	107.98	102.85	88.19	90.33	72.14	122.45
1500	107.47	91.98	108.04	102.91	87.98	90.53	72.18	122.49
1600	107.69	92.03	108.09	102.93		90.73		122.69
1700	107.89	92.06	108.13	102.96		90.92		122.77
1800	108.09	92.08	108.15	102.96		91.11		122.90
1900	108.28	92.10	108.16	102.96		91.29		123.02
2000	108.46	92.10	108.16	102.95		91.47		123.13
2100	108.63	92.09	108.15	102.94		91.65		123.22
2200	108.79	92.08	108.13	102.92		91.82		123.31
2300	108.95	92.05	108.03	102.87		91.98		123.40
2400	109.09	92.05	108.08	102.85		92.15		123.47
2500	109.23	92.02	108.05	102.81		92.31		123.54
2600	109.37	91.99	108.01	102.76				123.60
2700	109.50	91.96	107.96	102.72				123.66
2800	109.62	91.92	107.92	102.67				123.71
2900	109.73	91.88	107.87	102.62				123.76
3000	109.84	91.84	107.81	102.55				123.81
				Bond Properties				
$\nu$ , cm <sup>-1</sup>	4159	2813	2994	2951	982	2559	762	3704
$r_e$ , Å	0.7414	1.116	1.087	1.094	1.532	1.414	1.933	0.958

this less demanding case, while standard databases, columns 4 and 5, have an average discrepancy of 0.169 log unit between them. For comparison with thermodynamic  $\log(K_e)$ , Table 3 also shows  $\log(k_1/k_{-1})$ , obtained from the ratio of the rate constants for the forward and reverse reactions  $\text{CH}_3\text{-H} + \cdot\text{H} \rightleftharpoons \text{CH}_3\cdot + \text{H-H}$ , from two recommended<sup>17,18</sup> best three-parameter fits of available kinetic measurements for each reaction. In neither case is there good agreement with thermodynamic  $\log(K_e)$ .

Instead of comparing thermodynamic  $K_e$  values to ratios of calculated  $(k_1^*/k_{-1}^*)$ ,  $k_{-1}$  can be obtained from the calculated rate constant of the reverse reaction by  $k_1^*/K_e$  and compared to the independently obtained  $k_{-1}^*$ . The dashed lines in Figures 3 and 6 represent  $\ln(k_1^*/K_e)$ , calculated with  $K_e$  from Table 3, columns 4 and 5, respectively. A visual comparison of the two approaches for Figure 3, the more demanding case of methane, shows good agreement between  $k_{-1}^*$  and  $k_1^*/K_e$  in the range 400–2000 K, with some deviations appearing above and below this range. The more common exothermic or endothermic type of reaction is represented by the case of ethane in Figure 6, which shows very good agreement to 1500 K, above which point there are no measurements.

## Data

Heats of formation used for obtaining BDE values at different temperatures are from a NIST compilation,<sup>28</sup> except as follows. For C<sub>2</sub>H<sub>6</sub> and C<sub>2</sub>H<sub>5</sub><sup>•</sup>, they are from a NASA compilation,<sup>29</sup> which reflects a recent upward revision in BDE(C<sub>2</sub>H<sub>5</sub>-H). Heats of formation of propane and methyl bromide are calculated from (H - H<sub>298</sub>) available up to 1500 K, given in a NIST compilation.<sup>30</sup> Reported values of BDE-(OCH-H) at 300 K vary from 90.20 (1985 JANAF Tables)<sup>28</sup> to 89.80 (NIST-69)<sup>28</sup> to 88.11 (NASA).<sup>29</sup> We used the average, 89.3; the

temperature dependence of BDE is the same in all three sources. BDE values used at the various temperatures are given in Table 4, as are the other bond properties used in the calculation of  $E^*$ . Stretching frequencies are from Shimanouchi,<sup>31</sup> weighted for symmetric and asymmetric modes.<sup>12,32</sup> For the stretching frequency of C<sub>2</sub>H<sub>5</sub>-CH<sub>3</sub> we used 982 cm<sup>-1</sup>, the average of all isotopically substituted propanes;<sup>31</sup> the uncoupled C-C stretching frequency can also be calculated<sup>12,32</sup> from the BDE at 298 K by  $170(\text{BDE})^{1/2} - 617 = 986 \text{ cm}^{-1}$ , which is near enough to indicate that the observed vibrations are not highly coupled. In the case of CH<sub>3</sub>-Br, the observed C-Br stretching frequency is coupled to C-H bending vibrations and the uncoupled value was calculated<sup>12</sup> as  $170(\text{BDE})^{1/2} - 670 = 762 \text{ cm}^{-1}$ . Bond lengths are from the CRC Handbook.<sup>33</sup>

## Discussion

This work demonstrates that eq 10 successfully describes non-Arrhenius behavior for the hydrogen abstractions treated, in the temperature ranges examined. Equation 10 is successful with all three types of reactions: those that can be described by linear plots of  $\ln(k)$  vs  $1/T$  (Arrhenius behavior), by linear plots of  $\ln(k/T)$  vs  $1/T$  (Eyring's eq 3 with constant  $\Delta S^\ddagger$ ,  $\Delta H^\ddagger$ , and  $\kappa$ ), or by the three-parameter equation (Kooij's eq 1 with values of  $n$  as high as 6). While the three-parameter eq 1 provides a convenient and flexible way of fitting data, there is a funda-

(30) Stein, S. E., *Software Structures and Properties*, Version 2.0 in NIST Standard Reference Database Number 25, January 1994, National Institute of Standards and Technology: Gaithersburg, MD. Data evaluated by S. G. Lias, J. F. Liebman, R. D. Levin, and S. A. Kafafi.

(31) Shimanouchi, T. *Tables of Molecular Vibrational Frequencies*, National Standard Reference Data Series No. 39; U.S. National Bureau of Standards, U.S. Government Printing Office: Washington, DC, 1972.

(32) Zavitsas, A. A. *J. Phys. Chem.* **1987**, *91*, 5573.

(33) *Handbook of Chemistry and Physics*, 74th ed.; Lide, D. R., Ed.; CRC Press: Boca Raton, FL, 1993–1994.



mental difference in the  $E^*$  calculation. The form of eq 1 requires either no curvature ( $n = 0$ ) or a smoothly and monotonically increasing degree of curvature with increasing temperature ( $n > 0$ ) in plots of  $\ln(k)$  vs  $1/T$ . The results obtained here indicate that a monotonically increasing degree of curvature is not always obtained, as is most clearly visible in Figure 4 and as demonstrated for various domains of Figures 2 and 3, where temperature-dependent changes in  $\Delta H_{\text{rxn}}$  alone must produce exactly such effects. Scatter in the data does not allow a clear experimental demonstration of this behavior, leaving the possibility of artifacts due to inaccurate values for the temperature dependence of BDE given in the databases used.<sup>28–30</sup> We note that variational TS theory (ICVT) also can produce nonmonotonic changes in curvature (prior to application of tunneling corrections).<sup>4a</sup>

Agreement of  $\ln(k^*)$  with experiment in Figures 1–8, the results of Table 3, and Figures 3 and 6 demonstrate that the entropy of activation changes little in these cases. The quantities  $\Delta H^\ddagger$  and  $\Delta S^\ddagger$  are not independent of each other,<sup>2</sup> being related via  $\Delta C_p^\ddagger$ , and are subject to the well-known “compensation effect”. Nevertheless, setting  $\Delta S^\ddagger = \text{constant}$  is a good approximation.

van't Hoff was correct in considering that the energy change in a reaction may not be independent of temperature and that this would affect  $E$ , eq 2. However, this work demonstrates that change in  $\Delta H_{\text{rxn}}$  is not the only major factor affecting the temperature dependence of the enthalpy of activation. Triplet repulsion,<sup>3</sup>  $E(X-Y)^\ddagger$ , is also temperature dependent and plays a major role in the calculation of  $E^*$ , even though X–Y is neither reactant nor product.

As an illustration of the magnitudes of the terms comprising  $E^*$ , we examine the nearly thermoneutral reaction  $\text{H}_3\text{C}-\text{H} + \cdot\text{H}$ . At the TS (300 K), the calculation shows that bonding in  $\text{CH}_3-\text{H}$  has decreased by  $4.12 \text{ kcal mol}^{-1}$  to 100.70 (the H–H bond has been formed to the same extent), triplet repulsion between  $\text{H}_3\text{C}$  and the terminal hydrogen is 16.87,  $E_{\text{R}} = -10.60$ , and  $\Delta(\text{ZPE}) = 0.83$ .  $E^* = 4.12 + 16.87 - 10.6 + 0.83 = 11.22$ . Considering the strongly endothermic reaction  $\text{H}_3\text{C}-\text{H} + \cdot\text{Br}$  at the TS (300 K), bonding in  $\text{H}_3\text{C}-\text{H}$  has decreased by  $19.07 \text{ kcal mol}^{-1}$  to 85.75 (the H–Br bond has formed to the same extent), triplet repulsion is 11.97,  $E_{\text{R}}$  is  $-12.0$ , and  $\Delta(\text{ZPE}) = -0.31$ .  $E^* = 19.07 + 11.97 - 12.00 - 0.31 = 18.73$ . The extent of bond breaking and bond making at the TS (300 K) for the various reactions treated here is shown below. Each dash represents partial bonding of  $1 \text{ kcal mol}^{-1}$  less than the BDE of the bond.

$\Delta H = -15.0$	H-H-----OH
$\Delta H = -14.5$	OCH-H-----H
$\Delta H = -4.3$	$\text{C}_2\text{H}_5\text{---H-----CH}_3$
$\Delta H = -3.7$	$\text{C}_2\text{H}_5\text{---H-----H}$
$\Delta H = 0.6$	$\text{CH}_3\text{---H----H}$
$\Delta H = 16.7$	$\text{CH}_3\text{-----H--Br}$
$\Delta H = 17.3$	$\text{H-----H---Br}$

The representation above is a restatement of the 1955 Hammond postulate,<sup>34</sup> but in more quantitative fashion, and is

a direct consequence of the requirement of the  $E^*$  calculation that the partial strengths of the bonds broken and made be equal at the TS.

Calculated bond-stretching and bond-forming distances at the TS change with the temperature-dependent  $\Delta H_{\text{rxn}}$ , as might be expected. A large variation in  $\Delta H_{\text{rxn}}$  is found in the reaction  $\text{C}_2\text{H}_5-\text{H} + \cdot\text{H}$ , where  $\Delta H_{\text{rxn}}$  goes from  $-3.7 \text{ kcal mol}^{-1}$  at 300 K to  $-7.3$  at 3000 K. The  $\text{C}_2\text{H}_5-\text{H}$  bond length at the TS is  $0.022 \text{ \AA}$  shorter at 3000 K than at 300 K, and the H–H bond length is correspondingly  $0.033 \text{ \AA}$  longer. Changes with temperature in the location of the bottleneck have been found by other calculations as well.<sup>3</sup>

All exothermic reactions studied by the  $E^*$  calculation, previously<sup>12</sup> and in this work, have shown that triplet repulsion exceeds  $E^*$  and, therefore, must be a major cause for the very existence of energy barriers to chemical reactions.

The a priori approach described here provides insight into the major factors controlling enthalpies of activation for hydrogen abstractions by radicals. It is limited in that it does not provide rate constants since the value of  $B$  in eq 10 must be obtained from experiment at one temperature. Rigorous quantum dynamics provide rate constants but require detailed information about the potential energy surface and are often difficult and expensive to apply. Our approach requires information only about bonds in three stable molecules and provides a simpler, more intuitive and inexpensive calculation of the temperature dependence of rate constants. It allows extrapolation of low-temperature rate constant measurements to the high temperatures of interest in combustion. Also, this approach is not applicable to other types of reactions, such as additions, cyclizations, carbene insertions, etc.

The computer program used for the calculation of  $E^*$  is available on request from ZAVITSAS@AURORA.LIUNET.EDU. The program ESTAR, Version 4, is written in BASIC for PC and executes in less than 1 s. Should a user change the program in any way, we request that the changed version not be identified as ESTAR.

## Conclusions

This work focuses on the enthalpy term of the relationship between rate constants and temperature and demonstrates that changes in  $E^*$  describe well the variety of experimentally obtained curvatures in plots of  $\ln(k)$  vs  $1/T$  for the reactions and the temperature ranges examined. Changes in  $E^*$  are caused by changes in  $\text{BDE}(\text{X}-\text{H})$ ,  $\text{BDE}(\text{H}-\text{Y})$ , and  $\text{BDE}(\text{X}-\text{Y})$ . The Eyring equation adequately describes curvatures of  $\ln(k)$  vs  $1/T$  plots for eight typical hydrogen abstractions when  $\Delta H^\ddagger$  is estimated by the  $E^*$  calculation, with BDE values appropriate to each temperature and constant  $\Delta S^\ddagger$  and  $\kappa$ . A major factor affecting  $E^*$  is the magnitude of triplet repulsion between the terminal atoms of a reacting three-electron system, consistent with the London equation.

**Acknowledgment.** Partial support by the Research Time Committee and by the Trustees of LIU is gratefully acknowledged.

JA973698Y